A sensitive, single-tube assay to measure the enzymatic activities of influenza RNA polymerase and other poly(A) polymerases: application to kinetic and inhibitor analysis

Lisa Hooker, Rebecca Strong, Ralph Adams, Balraj Handa[1], John H. Merrett[1], Joseph A. Martin[1] and Klaus Klumpp*

Department of Biology and [1]Department of Chemistry, Roche Discovery Welwyn, 40 Broadwater Road, Welwyn Garden City, Hertfordshire AL7 3AY, UK

ABSTRACT

We describe a fast and robust new assay format to measure poly(A) polymerase (PAP) activity in a microtiter plate format. The new assay principle uses only natural nucleotide triphosphates and avoids a labour-intensive filtration step. A coupled enzymatic system combining PAP and reverse transcriptase forms the basis of the assay. The PAP generates a poly(A) tail on a RNA substrate and the reverse transcriptase is used to quantify the polyadenylated RNA by extension of a biotinylated oligo-dT primer. We demonstrate the principle of the assay using influenza virus RNA polymerase and yeast PAP as examples. A specific increase in the K_m value for ATP and the observation of burst kinetics in the polyadenylation dependent, but not in the polyadenylation independent, assay suggest that a rate limiting step of influenza polymerase activity occurs after transcription elongation. Yeast PAP was used to validate the assay as an example of a template independent PAP. The new yeast PAP assay was ~100-fold more sensitive than the conventional TCA precipitation assay for yeast PAP, but the kinetic analysis of the PAP reaction gave similar results in both assays. The two enzymes show important differences with respect to inhibition by 3′-deoxy-ATP. Whereas the K_i value for 3′-deoxy-ATP (105–117 μM) is similar to the K_m value for ATP (186 μM) in the case of influenza RNA polymerase, the K_i value for 3′-deoxy-ATP (0.4–0.6 μM) is ~100-fold lower than the K_m value for ATP (50 μM) in the case of yeast PAP.

INTRODUCTION

Polyadenylation is an important feature of mRNA recognition in eukaryotic cells. Poly(A) tails on mRNA molecules are involved in the regulated processes of nuclear export, translation and mRNA degradation (1–6). Polyadenylation of mRNA molecules also occurs in prokaryotes and contributes to the regulation of mRNA stability (7). The regulated process of mRNA polyadenylation is carried out within a complex of many protein subunits in close coordination with cleavage site recognition and endonucleotic cleavage of nascent mRNA 3′-ends (8–10). Eukaryotic poly(A) polymerases (PAP) are monomeric proteins that contain the catalytic sites for the synthesis of poly(A) tails. Isolated PAP proteins are catalytically active, but are unable to recognise specific polyadenylation sites on mRNA precursor molecules. Instead, they can use most RNA molecules as primers to generate poly(A) tails in a template independent fashion (11–13).

Poly(A) tails can also be generated in a template dependent manner. This mechanism of polyadenylation is thought to be used by a number of RNA viruses including influenza virus, a RNA virus with a genome of single-stranded RNA segments (14). Replication of the genomic RNA and production of influenza virus mRNA occurs in the nucleus of infected cells. A virus encoded RNA template dependent RNA polymerase harbours the catalytic functions required for transcription and replication of the viral genome. The functional unit of viral transcription and replication is a ribonucleoprotein particle (RNP). The RNP consists of the polymerase bound to a genomic RNA segment, with multiple copies of nucleoprotein bound to the single-stranded RNA (14). The influenza virus polymerase produces capped and polyadenylated mRNAs to ensure their efficient nuclear export and translation in the host cells. In contrast to eukaryotic polyadenylation by PAP, influenza virus appears to use a template dependent mechanism of generating poly(A) tails (15). The influenza virus polymerase contains an associated endonuclease activity, which is required to generate a capped RNA primer from a capped RNA precursor molecule. The polymerase then initiates transcription on the capped RNA primer. A transition between transcription initiation and elongation is apparent early in the transcription process as indicated by an accumulation of short, abortive transcripts, before the polymerase becomes highly processive (16). During transcription elongation the polymerase extends the capped primer until it reaches a termination

*To whom correspondence should be addressed. Tel: +44 1707 361085; Fax: +44 1707 332053; Email: klaus.klumpp@roche.com

signal, a conserved oligo(U) stretch close to the 5′-end of the viral RNA template. The influenza polymerase then adds a poly(A) tail to the 3′-end of the nascent viral mRNA by reiteratively copying the oligo(U) stretch (15,17–19). In accordance with this mechanism, the oligo(U) stretch has been shown to be essential for the expression of a reporter gene from viral RNA analogues (15,20,21).

Importantly, influenza virus polymerase has been shown to interact strongly with a conserved viral genomic RNA (vRNA) 5′-end sequence just upstream of the conserved oligo(U) stretch (22–25). This finding supports the model that influenza polymerase remains bound to the conserved 5′-end during transcription while copying the vRNA from the 3′-end. In this way, once transcription reaches the oligo(U) stretch, the polymerase's concomitant interaction with the proximal conserved 5′-end could cause continuous polymerase slippage and reiterative copying of the oligo(U) track (15,19,20,22,23,26,27).

Several assay types have been used to study RNA polymerase and PAP activities *in vitro*, but most require multiple steps and are labour-intensive. In addition, for radioactive read-out assays, the concentration of the labelled substrate is usually suboptimal. Many homogeneous, single-tube assay formats rely on modified nucleotides or primers, which can influence the interaction of substrate with the polymerase protein under study. We have therefore developed a single-tube PAP assay, which uses only natural substrates at optimal concentrations and is adaptable to high throughput kinetic or screening analysis. For yeast PAP the assay is significantly more sensitive and robust than a comparable acid-precipitation and filtration based protocol. In the case of influenza virus polymerase, it is the first single-tube assay that encompasses all enzymatic activities including cap-dependent endonuclease, transcription and polyadenylation activities in a single reaction read-out.

MATERIALS AND METHODS

Materials

Influenza virus A/PR/8/34 RNPs were prepared from purified influenza virus particles on glycerol gradients as described (28). Protein preparations were analysed for purity by SDS–PAGE and protein concentration was estimated from OD measurements and Bradford analysis as described (28). Yeast PAP and streptavidin coated scintillation proximity assay (SPA) beads were from Amersham Pharmacia Biotech. Alfalfa mosaic virus (AMV) RNA was kindly provided by Prof. John Bol (Leiden University, The Netherlands). Biotinylated oligo(dT)$_{20}$ and Expand reverse transcriptase were from Roche Molecular Biochemicals. Rabbit globin mRNA was purchased from Life Technologies.

Enzyme assays

TCA precipitation assay. The TCA precipitation assay for influenza polymerase was modified from a previously published protocol (16). Unless stated otherwise in the figures, 0.5 µg purified RNP protein (1.7 nM) was incubated for 90 min at 30°C in a final reaction mixture containing 10 ng/µl AMV RNA, 500 µM ATP, 50 µM CTP, 50 µM GTP, 2 µM UTP and 0.44 µM [^{3}H]UTP in buffer A (50 mM Tris–HCl pH 8,

100 mM KCl, 5 mM MgCl$_2$, 5 mM DTT, 0.2 mg/ml BSA). The reaction was typically carried out in 50 µl total volume on 96-well filter plates (Millipore MADV-NOB plates). The reaction was stopped by the addition of 50 µl 20% cold TCA. After a 30 min incubation at 4°C, the plates were washed under vacuum five times with 10% TCA and once with 70% ethanol, then dried and counted in a Wallac microbeta scintillation counter.

Yeast PAP assays were usually run on 96-well filter plates using 20–100 U of enzyme in 50 µl total volume in buffer Y (20 mM Tris–HCl pH 7, 50 mM KCl, 0.7 mM MnCl$_2$, 0.2 mM EDTA, 100 µg/ml BSA, 10% glycerol) containing 5 ng/µl AMV RNA and 0.54 µM [^{3}H]ATP. Incubation was for 30 min at 30°C, TCA precipitation and analysis as described above. Yeast PAP (1 U) catalyses the incorporation of 1 pmol of ATP into acid insoluble form in 1 min at 37°C using poly(A) of length 100 nt as a primer.

Poly(A) SPA assay. The influenza polymerase assay was carried out on ISO 96-well plates (Perkin Elmer Life Sciences) by incubating 1–5 nM RNP protein in buffer B (50 mM Tris–HCl pH 8, 40 mM KCl, 3 mM MgCl$_2$, 5 mM DTT) with 5 ng/µl AMV RNA, 500 µM ATP, 50 µM each CTP, GTP, UTP and 10% DMSO in 50 µl total volume at 30°C for 90 min. An aliquot of 10 µl of Expand RT poly(A) detection mix [50 U Expand RT and 1.8 µM oligo(dT)$_{20}$, 60 µM each dATP, dCTP, dGTP and 0.15 µM [^{3}H]TTP in buffer B] was then added and the plate transferred to 42°C for 60 min. The reactions were stopped and the product captured by adding 50 µl streptavidin coated SPA beads at 10 mg/ml, which had been reconstituted in 100 mM NaCl, 10 mM Tris–HCl pH 8, 75 mM EDTA and 0.02% sodium azide. The samples were measured on the plates in a Wallac microbeta scintillation counter.

Yeast PAP assays were performed essentially as described for influenza polymerase, except that the reactions were carried out in buffer Y and the plates incubated at 30°C for 30 min, before adding the Expand RT poly(A) detection mix. Typically, 0.08–0.2 U of enzyme were used in 50 µl reactions. The analysis of products by scintillation proximity was as described for influenza polymerase.

Data analysis, poly(A) SPA assay. The background signal in the absence of RNP or PAP was measured in triplicate per plate and the averaged value was subtracted from the triplicate averaged enzyme signal before further data analysis. K_m values for the polymerase substrates were determined by non-linear fitting of hyperbolic progress curves to the data using Sigma-Plot 5.0. K_i values were determined by non-linear fitting of dose response curves to the data using the kinetic constants determined previously using SigmaPlot 5.0 or Microsoft Excel 97. Alternatively, K_i values were determined using linear Dixon plot analysis (after plotting 1/activity versus inhibitor concentration).

Influenza polymerase transcription elongation assay. The transcription reactions were done in the same way as described previously (29) using 1 nM RNP, 0.1 nM cap-labelled G11 RNA, 10 µM CTP, GTP and UTP and 100 µM ATP. The reaction products were analysed by 20% urea–polyacrylamide gel electrophoresis.
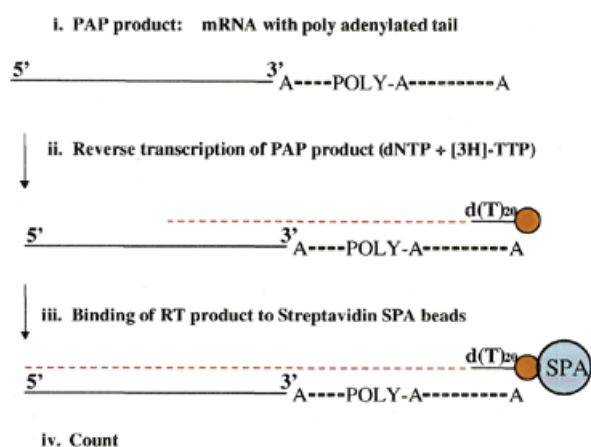
Figure 1. Poly(A) SPA assay principle. The PAP enzyme generates a polyadenylated RNA molecule (step i). Biotinylated oligo-d(T)$_{20}$ oligonucleotide hybridises to the poly(A) tail and is reverse transcribed by Expand-RT in the presence of dNTPs and [^{3}H]TTP (step ii). The radioactive, biotinylated RT product binds to streptavidin coated SPA beads (step iii) and can be directly measured by scintillation counting (step iv).

Figure 2. Dependence of the poly(A) SPA assay on polyadenylated RNA. RNA molecules were reverse transcribed by Expand-RT under the conditions of the poly(A) SPA assay format. The assay signal increased with increasing levels of polyadenylated globin mRNA (black triangles). Only low levels of signal were generated with non-polyadenylated RNA, AMV RNA (black circles). Background levels of signal were generated in the absence of biotinylated oligo-d(T)$_{20}$ with globin mRNA (white triangles) or AMV RNA (white circles). The inset shows the same samples measured at higher RNA concentration. RNA concentrations were 0, 3.03, 6.06, 15.15, 30.3, 60.6, 90.9, 121.2, 181.8 and 242.4 nM AMV RNA and 0, 0.6, 1.51, 3.015, 6.03 and 15.08 nM globin mRNA.

RESULTS

Poly(A) SPA assay principle

The principle of the SPA assay format for poly(A) polymerases is described in Figure 1. The polymerase uses ATP to generate a poly(A) tail on a RNA molecule provided in the reaction (step i). In the case of influenza RNP, the polymerase will generate the RNA molecule as well as the poly(A) tail from a capped RNA primer in the presence of all four NTPs. Biotinylated oligo(dT)$_{20}$ oligonucleotide hybridises to the poly(A) tail under the assay conditions and is elongated by reverse transcriptase in the presence of dNTPs, one of which is radioactively labelled (step ii). The reverse transcription reaction is stopped by the addition of EDTA and streptavidin coated SPA beads (step iii). The amount of reverse transcriptase product is then directly determined by scintillation counting, as the SPA technology does not require the separation of unincorporated substrate from the product (30). The polyadenylated RNA generated by the PAP serves as a template for the reverse transcription by Expand-RT. Therefore, the radioactivity incorporated into the reverse transcriptase product is directly related to the amount of poly(A) RNA from the first part of the reaction. To verify this relationship we measured the reverse transcriptase reaction with SPA read-out in the presence of increasing amounts of polyadenylated rabbit globin mRNA. As expected, the RT-signal was directly related to the amount of globin mRNA in the assay (Fig. 2). The reverse transcription activity on RNA molecules lacking poly(A) tails was significantly lower under the optimised assay conditions (Fig. 2, AMV RNA), at concentrations of non-polyadenylated RNA up to 240 nM (Fig. 2, inset). Also, only background levels of RT activity were detected in the absence of biotinylated oligonucleotide (Fig. 2).
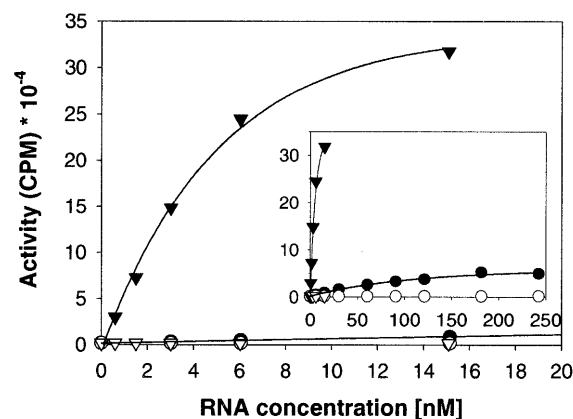
Influenza virus polymerase activity measured in the poly(A) SPA assay

Next we investigated the influence of poly(A) generating influenza polymerase on the signal in the coupled SPA assay. Influenza RNP was used as the source of polymerase enzyme. The RNP contains the polymerase bound to the genomic, viral template RNA. AMV RNA was used as a substrate for the RNP associated endonuclease activity. The endonuclease generates a primer RNA molecule from AMV RNA, which is then elongated by the influenza polymerase. Finally, the polymerase adds a poly(A) tail to the full-length transcripts of the genome. Figure 3A shows that the poly(A) dependent signal was directly related to the concentration of influenza RNP in the assay and to the incubation time. Under the conditions shown the specific activity increased linearly with time between 60 and 180 min (Fig. 3B). The SPA signal was ~10-fold lower in the absence of RNP. This background value was most likely due to low level unprimed reverse transcription on AMV RNA and was subtracted from the polymerase activities.

In the presence of saturating amounts of NTPs the influenza polymerase assay was linear with time for up to 5 h at 30°C (Fig. 3D). Interestingly, the back-extrapolation of the linear phase of the curve crossed the *x*-axis above the origin. This indicates that a burst of product formation occurs at early times in the reaction and precedes the slower, linear steady state phase measured at later time points. Rapid bursts in product formation are observed in enzyme reactions, when a step other than the chemical step in the reaction pathway limits enzyme turnover and reaction re-initiation. Reactions following burst kinetics are characterised by the fact that the amplitude of the burst is directly related to the enzyme concentration, because the burst in product formation is generated from a single reaction
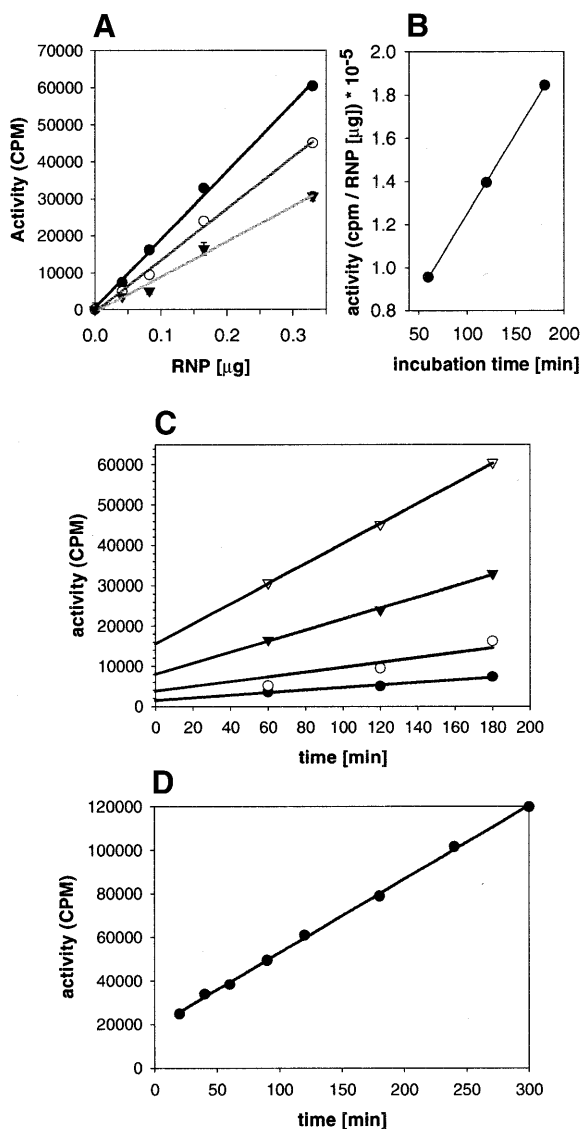
Figure 4. Primer extension by influenza polymerase is fast and processive. RNP (1 nM) was incubated with 0.1 nM capped 11mer primer RNA and incubated at 30°C for increasing lengths of time. The reactions were analysed on a 20% urea–PAGE gel. The black arrowhead shows the migration of the primer, the white arrowhead shows the migration of up to genome length transcripts accumulating near the top of the gel, indicated with T on the right. The numbers on the right of the gel indicate the sizes of RNA molecules in nucleotides. Lane 1, no RNP; lanes 2–8, incubation for 0, 5, 10, 30, 60, 90 and 120 min; lane 9, 0 min.

Figure 3. Burst kinetics of influenza polymerase activity in the polyadenylation dependent assay. Influenza RNA polymerase activity is linear with time and enzyme concentration in the poly(A) SPA assay. Cap dependent transcription reactions were initiated with AMV RNA and polyadenylation activity determined at different time points. (**A**) Transcription reactions in the presence of increasing concentration of influenza RNP incubated for 60 min (triangles), 120 min (white circles) or 180 min (black circles) at 30°C, before the addition of the Expand-RT poly(A) detection mix. (**B**) Replot of the specific activities determined in (A) relative to the incubation time. The specific activities increase linearly with time. (**C**) Replot of the activities observed in (A) with different amounts of RNP: 0.33 μg (white triangles), 0.165 μg (black triangles), 0.0825 μg (white circles) and 0.0413 μg (black circles). The y-intercepts and slopes are linearly related to the RNP concentration. (**D**) Time course of the influenza transcription–polyadenylation reaction using 0.6 μg RNP (2.14 nM).

initiation event. As shown in Figure 3C, the y-intercepts in the influenza polymerase reaction were linearly related to the RNP concentration, confirming burst kinetics of the complete transcription reaction. Burst kinetics were not observed in the TCA precipitation assay of influenza polymerase, in which the signal generated is not dependent on the generation of full-length RNA (see below).

The TCA precipitation procedure only captures transcription events up to the phase of transcription elongation. Therefore,
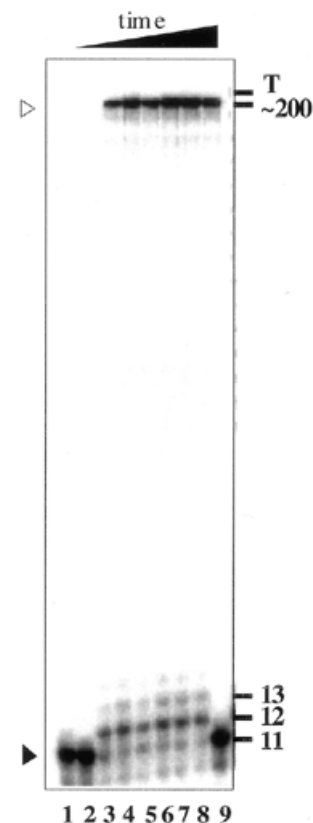
the burst kinetics observed in the polyadenylation dependent assay, which was absent in the TCA precipitation assay, suggested that a process at a stage later than transcription elongation was rate limiting in the complete influenza polymerase reaction. Consistent with this, a gel analysis of transcription elongation confirmed a high processivity of elongation by influenza polymerase and an elongation rate significantly higher than the steady state rate observed in the polymerase assay.

Figure 4 shows a transcription reaction initiated with a labelled and capped 11mer RNA primer in the presence of all four NTPs and enzyme excess. The primer was efficiently elongated by influenza polymerase. Most of the primer molecules were converted into long RNA transcripts within 10 min at 30°C. In addition, abortive transcripts of 12 and 13 nt (primer +1 nt and primer +2 nt) were produced, similar to previous observations (16). The influenza polymerase catalysed transcription elongation with high processivity as apparent from the absence of significant amounts of prematurely terminated transcripts in the area between 14 and ~200 nt transcript length resolved on the gel shown in Figure 4.

To further evaluate the new assay format, the K_m values for the NTP substrates of influenza polymerase were determined in the TCA and the SPA assay. The results are shown in Table 1. The K_m values determined in both assays for CTP, GTP and UTP were comparable, suggesting a good correlation between the two assay types. However, the K_m value for ATP in the polyadenylation dependent assay was ~15-fold higher than the K_m value for ATP in the poly(A) independent TCA assay.

Table 1. Influenza polymerase: comparison of K_m values for nucleotide triphosphates

	K_m (μM)			
	ATP	CTP	GTP	UTP
TCA precipitation[a]	12.3 (±1.05)	0.29 (±0.16)	1.70 (±0.32)	1.53 (±0.42)[b]
SPA assay[a]	186.0 (±3.32)	0.45 (±0.08)	1.32 (±0.24)	2.11 (±0.62)

[a]Cap dependent transcription reactions using AMV RNA as primer. Standard deviation calculated from $n = 3$ individual experiments.
[b]To determine the K_m of UTP in the filtermat assay, H^3-GTP and GTP was used in place of H^3-UTP and UTP at equivalent concentrations.

Yeast PAP activity measured in the poly(A) SPA assay

Yeast PAP was chosen as an example of a template independent PAP protein to test the assay principle. Similar incubation conditions and AMV RNA as the primer are described here to allow the comparison of results with the influenza RNA polymerase assay. However, other RNA molecules can replace AMV RNA in this assay. Figure 5A shows time courses of the polyadenylation reaction with three different concentrations of PAP (0.5, 0.2 and 0.08 U). Under these conditions the assay was linear with time up to 60 min at 30°C with 0.2 U and up to 120 min with 0.08 U PAP.

The titration of PAP in the assay gave rise to a sigmoidal curve with relatively increased PAP activity at higher protein concentrations (Fig. 5B). The inset in Figure 5B shows the exponential increase of activity at low concentrations of yeast PAP. The same non-linear enzyme concentration dependence was observed in the TCA assay and has also been described before for mammalian PAP (31,32). Because of the sigmoidal dependence of activity on PAP concentration, the K_m value for ATP was determined at 0.08 and 0.2 U of enzyme (Table 2). When 0.08 U of PAP were used, the K_m value for ATP was very similar to that previously reported with oligo(A) as a substrate (11). With 0.2 U PAP the K_m value for ATP was slightly higher. Overall, the results of the kinetic analysis of yeast PAP activity in the TCA and poly(A) SPA assay were comparable in most aspects examined. However, an important finding was that the sensitivity of the poly(A) SPA assay was significantly greater than that achieved in the TCA assay. The PAP levels required to give a signal in the dynamic range of the assay were >100-fold lower in the poly(A) SPA assay as compared to the TCA precipitation assay.

Inhibition of influenza polymerase and yeast PAP by cordycepin triphosphate

3′-Deoxy-ATP (cordycepin-TP) is a chain terminating inhibitor of PAPs. Since cordycepin-TP is efficiently incorporated by
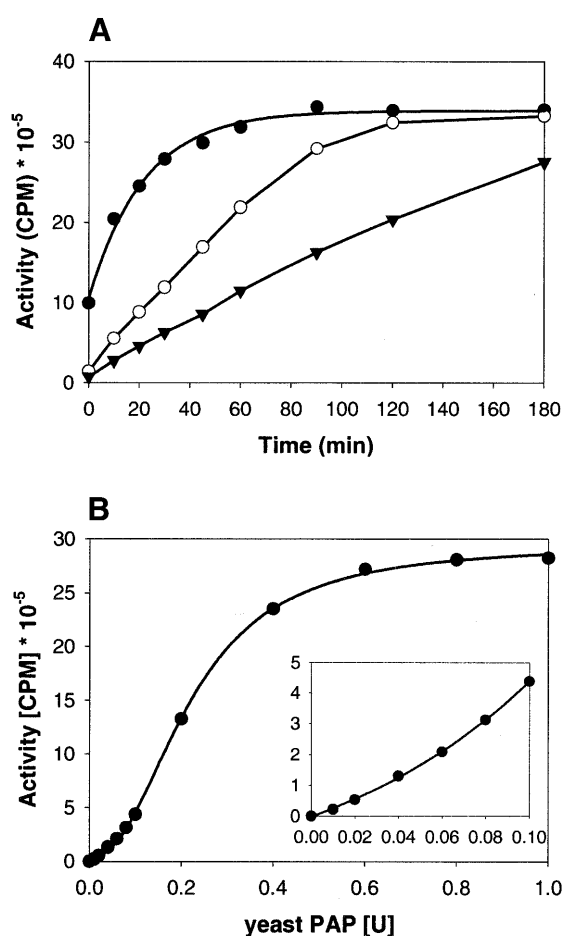

Figure 5. Kinetics of yeast PAP activity in the poly(A) SPA assay. The assay response in the presence of yeast PAP is linear with time, sigmoidal with enzyme concentration. (**A**) 0.5 U (black circles), 0.2 U (white circles) and 0.08 U (triangles) of yeast PAP was incubated with AMV RNA and ATP for the times indicated, before addition of the Expand-RT poly(A) detection mix. (**B**) Increasing concentrations of yeast PAP were incubated with AMV RNA and ATP for 30 min at 30°C before poly(A) quantification. The inset shows the exponential increase of signal at low concentrations of yeast PAP.

yeast PAP, it can be used as a tool to label RNA 3′-ends (33). To further validate the new assay format, we assessed the inhibition of influenza virus polymerase and yeast PAP by cordycepin-TP. As shown in Figure 6A, cordycepin-TP efficiently inhibited the activity of yeast PAP. The IC_{50} values were directly related to the concentration of ATP in the assay, indicating a competitive mechanism of inhibition. Competitive inhibition was also consistent with a linear graphical analysis of the data according to Dixon and Webb [Dixon plot (34)]. The K_i value for cordycepin-TP was determined by fitting dose-response curves to the data in Figure 6A using the K_m value for ATP as determined previously (Table 2). These values were identical within error to the K_i values determined from Dixon plot analysis. The K_i value for cordycepin-TP was significantly lower than the K_m value for ATP resulting in significant inhibition of yeast PAP at relatively low concentrations of cordycepin-TP. Importantly, the activity of Expand-RT was not reduced by up to 500 μM cordycepin-TP (Fig. 6B).

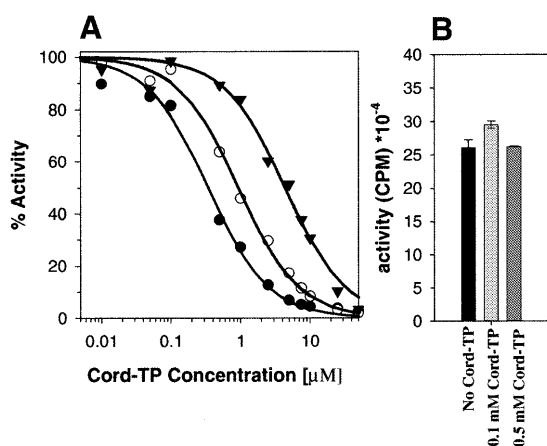Figure 7A shows the inhibition of influenza polymerase activity by cordycepin-TP at a concentration of 500 μM ATP

Figure 6. Inhibition of yeast PAP by cordycepin-TP. (**A**) Increasing amounts of cordycepin-TP were added to 0.2 U yeast PAP in the presence of AMV RNA and ATP at 50 µM (black circles), 100 µM (white circles) or 500 µM (triangles). Dose response curves were fitted to the data. (**B**) Globin mRNA was quantified with Expand-RT poly(A) detection mix in the absence (black bar) or presence of cordycepin-TP at 0.1 mM (light grey bar) or 0.5 mM (dark grey bar). Poly(A) detection was not inhibited by cordycepin-TP.

in the assay. Inhibition was also found to be competitive with ATP. In contrast to yeast PAP, the K_i value determined for inhibition by cordycepin-TP was similar to the K_m value for ATP with influenza polymerase (Table 2).

In order to verify that the poly(A) SPA assay for influenza polymerase was dependent on the endonuclease activity of RNP to provide the polymerase primer we analysed the impact of an endonuclease inhibitor on the assay. The diketobutanoic acid compound 2, described by Merck Research Laboratories (35) was resynthesised, purified and named Ro32-7804 (Fig. 7B). It has been shown that Ro32-7804 does not inhibit the RNA synthesis activity of influenza polymerase or reverse transcriptase at concentrations up to 1 mM, but it inhibited the endonuclease activity of influenza RNP with an IC_{50} of 0.5 µM (35; K.Klumpp and L.Hooker, unpublished results). Figure 7A shows that this compound was active as a potent inhibitor of influenza polymerase activity in the poly(A) SPA assay. This confirmed that the assay was also dependent on the endonuclease activity of influenza polymerase to generate a primer molecule for RNA synthesis.

DISCUSSION

The current study addressed the requirement for a fast, sensitive and robust assay format to measure the activity of PAPs. In addition, the new assay encompasses for the first time all enzymatic activities of the influenza virus polymerase in a
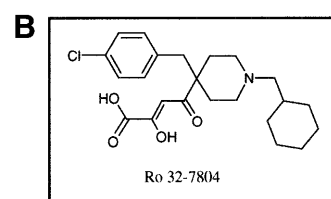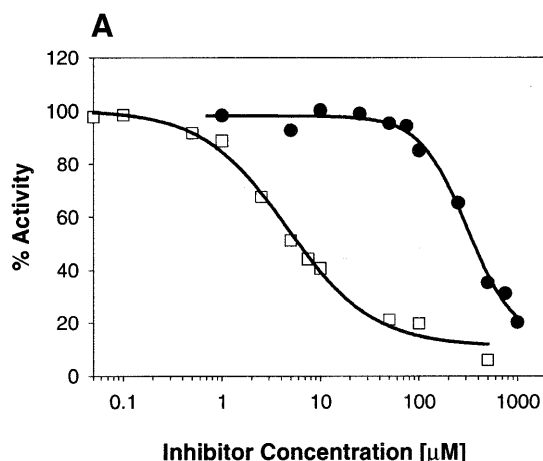

Figure 7. Inhibition of influenza polymerase by cordycepin-TP and Ro 32-7804. (**A**) Increasing concentrations of cordycepin-TP (circles) or the endonuclease inhibitor Ro 32-7804 (squares) were added to RNP enzyme in the poly(A) SPA assay format. Dose response curves for single binding sites were fitted to the data. The poly(A) SPA assay for the AMV RNA primed influenza virus transcription reaction is dependent on the endonuclease activity of RNP. (**B**) Structure of the endonuclease inhibitor Ro 32-7804, referred to as compound 2 by Tommassini *et al.* (35).

single-tube format, i.e. endonuclease activity, template dependent RNA synthesis activity and polyadenylation activity. The influenza polymerase signal in the poly(A) SPA assay was dependent on the endonuclease activity of influenza polymerase, as shown by the inhibition of signal generation in the presence of a selective endonuclease inhibitor. The assay was also dependent on the polyadenylation activity of influenza polymerase, because the signal from non-polyadenylated RNA in the assay was significantly below the signal from polyadenylated RNA.

Overall, the results obtained in the poly(A) SPA assay were very similar to those of the commonly used TCA precipitation assay. However, there were some interesting differences between the assay types. The poly(A) SPA assay was linear for up to 5 h under the assay conditions with saturating substrate concentrations, whereas the dynamic range of the TCA precipitation assay is generally limited by the concentration of

Table 2. Yeast PAP K_m values and enzyme inhibition by cordycepin 5′ triphosphate

K_m ATP (µM) yeast PAP		K_i (µM) yeast PAP		K_i (µM) influenza polymerase	
0.2 U[a]	0.08 U[a]	Non-linear fit[b]	Dixon plot[b]	Non-linear fit	Dixon plot
50 (±5)	123 (±26)	0.6 (±0.3)	0.4 (±0.1)	117 (±25)	105 (±15)

[a]Values determined from non-linear fitting of hyperbolic curves using AMV RNA as primer. Standard deviation calculated from $n = 2$ individual experiments.
[b]K_i values determined from reactions using 0.08 U yeast PAP.

labelled NTP and is difficult to keep saturated for long incubation times. Extrapolation of the linear phase in the poly(A) SPA assay gave a positive y-intercept dependent on the enzyme concentration, which suggested burst kinetics of the polymerase reaction. In contrast, the time courses in the TCA assay give no indication of a burst (36; L.Hooker and K.Klumpp, unpublished results). A major difference between the two assay types was that the poly(A) SPA assay was dependent on polyadenylation activity, whereas the TCA assay was not. Therefore, the observation of a burst exclusively in the poly(A) SPA assay suggested that the rate of the reaction was limited by a process after transcription elongation.

Another indication that transcription elongation was fast as compared to the influenza polymerase rate observed in the poly(A) SPA assay came from the analysis of transcription elongation rates on polyacrylamide gels. The gel analysis of transcription showed a fast and highly processive mechanism of elongation for the influenza polymerase. It has been shown previously that the endonuclease activity was limiting the rate in a transcription initiation assay under single turnover conditions, whereas product dissociation was most likely rate-limiting for endonuclease and transcription initiation reactions under multiple turnover conditions (28,37). The endonuclease reaction is unlikely to be responsible for the burst in the poly(A) SPA assay, because no burst is observed in the endonuclease dependent TCA assay. What else could then be the rate-limiting step in the influenza polymerase reaction? One candidate process is a possible conformational transition of RNP associated polymerase between an elongation and a polyadenylation form. It is currently unknown if the polymerase pauses, and how long the potential pause could be before the polymerase engages in a slippage reiterative polyadenylation activity (15). A second candidate process is reinitiation of transcription after transcription termination. Individual RNP molecules could go through cycles of repeated mRNA synthesis and transcription reinitiation after termination could be the rate-limiting process observed in the poly(A) SPA assay. Again, it is still unknown whether the influenza RNP is able to reinitiate transcription under *in vitro* conditions. Both of these possibilities demand further investigation.

Interestingly, the analysis of K_m values for the NTP substrates of influenza polymerase indicated a significant shift of the K_m value for ATP. This observation is consistent with a qualitative change of the polymerase complex and a possible conformational transition between processive RNA synthesis and reiterative poly(A) synthesis by slippage on a template oligo(U) stretch. The K_m values for NTPs other than ATP were similar in the poly(A) SPA and TCA assay formats. As shown before, the K_m values in capped RNA primed transcription reactions were lower than in transcription reactions primed with the dinucleotide ApG (16,38). Also consistent with previous results, the K_m value for ATP was ~10-fold greater than the K_m values of the other NTPs in the polyadenylation independent assay, probably due to a conformational change of the RNP during transcription initiation (16,38).

The poly(A) SPA assay was also shown to be a suitable new assay format for yeast PAP. The poly(A) SPA assay gave very similar results to the alternative TCA precipitation assay. In particular, an unusual non-linear increase in activity with increasing PAP concentration was observed in both assay types. Also, the K_m value for ATP was similar to previously reported values (11,31,32). This confirmed that under the optimised assay conditions, the assay signal truly reflected PAP dependent activity. Interestingly, the poly(A) SPA assay was significantly more sensitive than the TCA assay. The reason for this increase in sensitivity could be due to the use of a relatively long RNA primer, AMV RNA (964 nt), which increases the amount of labelled marker incorporated during reverse transcription.

The poly(A) SPA assay was further validated by the analysis of inhibition of polyadenylation by cordycepin-TP. The yeast PAP enzyme was significantly more sensitive to inhibition by cordycepin-TP as compared to influenza polymerase. The K_i value was >100-fold lower than the K_m value for ATP in the case of yeast PAP, whereas those constants were of similar magnitude in the case of influenza polymerase. The inhibition by cordycepin-TP was competitive with ATP for both enzymes under the assay conditions, whereas no inhibition was apparent with Expand-RT in the presence of up to 500 µM cordycepin-TP. Similar low K_i values for cordycepin-TP have been previously found with chromatin associated PAP from rat liver and purified template independent PAP of yeast and Vaccinia virus (39–41). The observation of relatively low K_i values for cordycepin-TP is most likely due to the fact that this nucleotide analogue is a chain terminator when incorporated into a nascent RNA molecule. In this respect, RNA synthesis and polyadenylation by influenza virus RNA polymerase was surprisingly resistant to inhibition by 3′-deoxy-ATP.

The analysis of cordycepin-TP inhibition illustrates the potential of the poly(A) SPA assay format to be widely applicable to screen for inhibitors of viral polymerases, which contain associated polyadenylation activity, or to PAPs of other infectious or parasitic organisms, for example pathogenic fungi and protozoa. It should be noted that in our example, cordycepin-TP did not inhibit the reverse transcriptase. However, other compounds from random screening approaches could inhibit this assay type by targeting the reverse transcriptase. Therefore, either parallel reverse trancriptase control reactions using globin mRNA in the assay, or a subsequent rescreen of inhibitors in a separate reverse transcriptase reaction, should be performed as a first step of inhibitor characterisation. The small amount of additional analysis required in this respect is in our experience more than compensated by the convenience and speed of the assay and the unique opportunity to screen all phases of the complete mRNA synthesis process in a single reaction.

Taken together, we have developed a new assay format for PAPs, which can replace the more labour intensive precipitation–filtration or filter binding protocols more commonly used with these enzymes. In contrast to direct radioactive and fluorescent assays, the poly(A) SPA assay allows the polyadenylation reaction to be performed in the presence of optimal concentrations of substrates, and a complete set of natural substrates can be used, rather than substrates modified with large tagging groups. The assay reproduced known features of the reaction kinetics of two unrelated enzymes, influenza RNA polymerase and yeast PAP. Analysis of reaction kinetics in the new assay suggests a previously undetected rate-limiting step, which occurs after transcript elongation with influenza RNA polymerase on RNP particles. For yeast PAP, the new assay format was found to be significantly more sensitive than commonly used alternative assays.

REFERENCES

1. Beelman,C.A. and Parker,R. (1995) Degradation of mRNA in eukaryotes. *Cell*, **81**, 179–183.
2. Sachs,A.B., Sarnow,P. and Hentze,M.W. (1997) Starting at the beginning, middle and end: translation initiation in eukaryotes. *Cell*, **89**, 831–838.
3. Wahle,E. and Ruegsegger,U. (1999) 3′-end processing of pre-mRNA in eukaryotes. *FEMS Microbiol. Rev.*, **23**, 277–295.
4. Tucker,M. and Parker,R. (2000) Mechanisms and control of mRNA decapping in *Saccharomyces cerevisiae*. *Annu. Rev. Biochem.*, **69**, 571–595.
5. Stutz,A., Conne,B., Huarte,J., Gubler,P., Volkel,V., Flandin,P. and Vassalli,J.D. (1998) Masking, unmasking and regulated polyadenylation cooperate in the translational control of a dormant mRNA in mouse oocytes. *Genes Dev.*, **12**, 2535–2548.
6. Conne,B., Stutz,A. and Vassalli,J.D. (2000) The 3′ untranslated region of messenger RNA: a molecular 'hotspot' for pathology? *Nat. Med.*, **6**, 637–641.
7. Coburn,G.A. and Mackie,G.A. (1999) Degradation of mRNA in *Escherichia coli*: an old problem with some new twists. *Prog. Nucleic Acid Res. Mol. Biol.*, **62**, 55–108.
8. Minvielle-Sebastia,L. and Keller,W. (1999) mRNA polyadenylation and its coupling to other RNA processing reactions and to transcription. *Curr. Opin. Cell Biol.*, **11**, 352–357.
9. Keller,W. and Minvielle-Sebastia,L. (1997) A comparison of mammalian and yeast pre-mRNA 3′-end processing. *Curr. Opin. Cell Biol.*, **9**, 329–336.
10. Shatkin,A.J. and Manley,J.L. (2000) The ends of the affair: capping and polyadenylation. *Nat. Struct. Biol.*, **7**, 838–842.
11. Lingner,J., Radtke,I., Wahle,E. and Keller,W. (1991) Purification and characterization of poly(A) polymerase from *Saccharomyces cerevisiae*. *J. Biol. Chem.*, **266**, 8741–8746.
12. Wahle,E. (1991) Purification and characterization of a mammalian polyadenylate polymerase involved in the 3′ end processing of messenger RNA precursors. *J. Biol. Chem.*, **266**, 3131–3139.
13. Lingner,J. and Keller,W. (1993) 3′-end labeling of RNA with recombinant yeast poly(A) polymerase. *Nucleic Acids Res.*, **21**, 2917–2920.
14. Lamb,R.A. and Krug,R.M. (1996) Orthomyxoviridae: the viruses and their replication. In Fields,B.N., Knipe,D.M. and Howley,P.M. (eds), *Fields Virology*. Lippincott-Raven Publishers, Philadelphia, Vol. I, pp. 1353–1395.
15. Poon,L.L., Pritlove,D.C., Fodor,E. and Brownlee,G.G. (1999) Direct evidence that the poly(A) tail of influenza A virus mRNA is synthesized by reiterative copying of a U track in the virion RNA template. *J. Virol.*, **73**, 3473–3476.
16. Klumpp,K., Ford,M.J. and Ruigrok,R.W. (1998) Variation in ATP requirement during influenza virus transcription. *J. Gen. Virol.*, **79**, 1033–1045.
17. Desselberger,U., Racaniello,V.R., Zazra,J.J. and Palese,P. (1980) The 3′ and 5′-terminal sequences of influenza A, B and C virus RNA segments are highly conserved and show partial inverted complementarity. *Gene*, **8**, 315–328.
18. Robertson,J.S. (1979) 5′ and 3′ terminal nucleotide sequences of the RNA genome segments of influenza virus. *Nucleic Acids Res.*, **6**, 3745–3757.
19. Robertson,J.S., Schubert,M. and Lazzarini,R.A. (1981) Polyadenylation sites for influenza virus mRNA. *J. Virol.*, **38**, 157–163.
20. Luo,G.X., Luytjes,W., Enami,M. and Palese,P. (1991) The polyadenylation signal of influenza virus RNA involves a stretch of uridines followed by the RNA duplex of the panhandle structure. *J. Virol.*, **65**, 2861–2867.
21. Li,X. and Palese,P. (1994) Characterization of the polyadenylation signal of influenza virus RNA. *J. Virol.*, **68**, 1245–1249.
22. Tiley,L.S., Hagen,M., Matthews,J.T. and Krystal,M. (1994) Sequence-specific binding of the influenza virus RNA polymerase to sequences located at the 5′ ends of the viral RNAs. *J. Virol.*, **68**, 5108–5116.
23. Fodor,E., Pritlove,D.C. and Brownlee,G.G. (1994) The influenza virus panhandle is involved in the initiation of transcription. *J. Virol.*, **68**, 4092–4096.
24. Hagen,M., Chung,T.D., Butcher,J.A. and Krystal,M. (1994) Recombinant influenza virus polymerase: requirement of both 5′ and 3′ viral ends for endonuclease activity. *J. Virol.*, **68**, 1509–1515.
25. Klumpp,K., Ruigrok,R.W.H. and Baudin,F. (1997) Roles of the influenza virus polymerase and nucleoprotein in forming a functional RNP structure. *EMBO J.*, **16**, 1248–1257.
26. Poon,L.L., Pritlove,D.C., Sharps,J. and Brownlee,G.G. (1998) The RNA polymerase of influenza virus, bound to the 5′ end of virion RNA, acts in *cis* to polyadenylate mRNA. *J. Virol.*, **72**, 8214–8219.
27. Pritlove,D.C., Poon,L.L., Fodor,E., Sharps,J. and Brownlee,G.G. (1998) Polyadenylation of influenza virus mRNA transcribed *in vitro* from model virion RNA templates: requirement for 5′ conserved sequences. *J. Virol.*, **72**, 1280–1286.
28. Klumpp,K., Hooker,L. and Handa,B. (2001) Influenza virus endoribonuclease. *Methods Enzymol.*, **342**, in press.
29. Klumpp,K., Doan,L., Roberts,N.A. and Handa,B. (2000) RNA and DNA hydrolysis are catalyzed by the influenza virus endonuclease. *J. Biol. Chem.*, **275**, 6181–6188.
30. Cook,N.D. (1996) Scintillation proximity assay: a versatile high-throughput screening technology. *Drug Discov. Today*, **1**, 287–294.
31. Winters,M.A. and Edmonds,M. (1973) A poly(A) polymerase from calf thymus. *J. Biol. Chem.*, **248**, 4756–4762.
32. Rose,K.M., Morris,H.P. and Jacob,S.T. (1975) Mitochondrial poly(A) polymerase from a poorly differentiated hepatoma: purification and characteristics. *Biochemistry*, **14**, 1025–1032.
33. Lingner,J. and Keller,W. (1993) 3′-end labelling of RNA with recombinant yeast poly(A) polymerase. *Nucleic Acids Res.*, **21**, 2917–2920.
34. Dixon,M. and Webb,E.C.(1979) *Enzymes*. Longman Group Ltd, London, 3rd edn.
35. Tomassini,J., Selnick,H., Davies,M.E., Armstrong,M.E., Baldwin,J., Bourgeois,M., Hastings,J., Hazuda,D., Lewis,J., McClements,W., Ponticello,G., Radzilowski,E., Smith,G., Tebben,A. and Wolfe,A. (1994) Inhibition of cap (m7GpppXm)-dependent endonuclease of influenza virus by 4-substituted 2,4-dioxobutanoic acid compounds. *Antimicrob. Agents Chemother.*, **38**, 2827–2837.
36. Bishop,D.H.L., Obijeski,J.F. and Simpson,R.W. (1971) Transcription of the influenza ribonucleic acid genome by a virion polymerase. *J. Virol.*, **8**, 66–73.
37. Olsen,D.B., Benseler,F., Cole,J.L., Stahlhut,M.W., Dempski,R.E., Darke,P.L. and Kuo,L.C. (1996) Elucidation of basic mechanistic and kinetic properties of influenza endonuclease using chemically synthesized RNAs. *J. Biol. Chem.*, **271**, 7435–7439.
38. Stridh,S. and Datema,R. (1984) Mode of interference of trisodium phosphonoformate (INN: foscarnet sodium), with influenza virus mRNA synthesis. *Virology*, **135**, 293–296.
39. Rose,K.M., Bell,L.E. and Jacob,S.T. (1977) Specific inhibition of chromatin-associated poly(A) synthesis *in vitro* by cordycepin 5′-triphosphate. *Nature*, **267**, 178–180.
40. Horowitz,B., Goldfinger,B.A. and Marmur,J. (1976) Effect of cordycepin triphosphate on the nuclear DNA-dependent RNA polymerases and poly(A) polymerase from the yeast *Saccharomyces cerevisiae*. *Arch. Biochem. Biophys.*, **172**, 143–148.
41. Shuman,S. and Moss,B. (1988) Vaccinia virus poly(A) polymerase. *J. Biol. Chem.*, **263**, 8405–8412.